Influence of Tightly Bound Mg^{2+} and Ca^{2+}, Nucleotides, and Phalloidin on the Microsecond Torsional Flexibility of F-Actin†

Conrad A. Rebello and Richard D. Ludescher*

Department of Food Science, Rutgers, The State University, New Brunswick, New Jersey 08901-8520

Received May 26, 1998; Revised Manuscript Received July 28, 1998

ABSTRACT: To better understand the relationship between structure and molecular dynamics in F-actin, we have monitored the torsional flexibility of actin filaments as a function of the type of tightly bound divalent cation (Ca^{2+} or Mg^{2+}) or nucleotide (ATP or ADP), the level of inorganic phosphate and analogues, KCl concentration, and the level of phalloidin. Torsional flexibility on the microsecond time scale was monitored by measuring the steady-state phosphorescence emission anisotropy (r_{FA}) of the triplet probe erythrosin-5-iodoacetamide covalently bound to Cys-374 of skeletal muscle actin; extrapolations to an infinite actin concentration corrected the measured anisotropy values for the influence of variable amounts of rotationally mobile G-actin in solution. The type of tightly bound divalent cation modulated the torsional flexibility of F-actin polymerized in the presence of ATP; filaments with Mg^{2+} bound ($r_{FA} = 0.066$) at the active site cleft were more flexible than those with Ca^{2+} bound ($r_{FA} = 0.083$). Filaments prepared from G-actin in the presence of MgADP were more flexible ($r_{FA} = 0.051$) than those polymerized with MgATP; the addition of exogenous inorganic phosphate or beryllium trifluoride to ADP filaments, however, decreased the filament flexibility (increased the anisotropy) to that seen in the presence of MgATP. While variations in KCl concentration from 0 to 150 mM did not modulate the torsional flexibility of the filament, the binding of phalloidin decreased the torsional flexibility of all filaments regardless of the type of cation or nucleotide bound at the active site. These results emphasize the dynamic malleability of the actin filament, the role of the cation−nucleotide complex in modulating the torsional flexibility, and suggest that the structural differences that have previously been seen in electron micrographs of actin filaments manifest themselves as differences in torsional flexibility of the filament.

F-Actin, an asymmetric polymer found in all eukaryotic cells, is an essential structural and contractile element involved in cellular functions as diverse as cell locomotion, cell division, maintenance of specific cellular shape, and muscle contraction (*1*). The structure of actin is known at atomic resolution from X-ray diffraction of complexes of skeletal α-actin with DNAase I (*2*) and with segment 1 of gelsolin (*3*) and of *β*-actin with profilin (*4*). Actin is a 42 kDa globular protein folded into distinct domains separated by a deep cleft. The actin filament (diameter ≅ 90 Å) can be described as a two-start, right-handed helix. A model of the filament at atomic resolution was generated by fitting the actin−DNAase I structure to low-resolution X-ray fiber diffraction patterns from oriented F-actin gels (*5*, *6*). This model now forms the basis for molecular interpretations of F-actin structure and function (*7*−*10*) and appears to be consistent with other data on filament structure (*5*).

Actin contains a single high-affinity ($K_d \approx 10^{-8}$ M for both Ca^{2+} and Mg^{2+}) (*11*) divalent cation binding site which has been located at the bottom of the deep cleft between the large and small domains. The nucleotide is also bound in this cleft, and interactions between the cation and the nucleotide phosphates indicate that cations bound to the high-affinity site are actually bound to the nucleotide. Under cellular conditions, the cation is Mg^{2+}, but most standard actin preparations isolate Ca^{2+}-actin (*11*). The nature of the divalent cation bound to the nucleotide at this site influences the large-scale structure and dynamics of F-actin. Several studies have demonstrated that the structure of the actin filament can be altered by varying either the type of tightly bound divalent cation (Ca^{2+} or Mg^{2+}) (*9*, *10*, *12*−*14*) or the nucleotide (ADP or ATP) (*15*) that is present in monomeric G-actin prior to polymerization. On the basis of these structural differences, differences in the bending flexibility of actin filaments have been proposed. However, when the bending flexibility of actin filaments which differed in the type of tightly bound divalent cation was measured directly (*16*) or inferred from persistence length measurements (*17*), these predictions were not fulfilled. Similarly, when the bending flexibility of actin filaments was determined as a function of the bound nucleotide (ATP or ADP) the data have either affirmed (*18*) or refuted (*10*, *17*, *19*) the predictions of the structural studies. Such apparently contradictory results suggest that our understanding of the manner in which the structural changes in F-actin manifest themselves as flexibility changes is incomplete.

† This work was supported by a grant to R.D.L. from the Muscular Dystrophy Association and by a graduate assistantship awarded to C.A.R. from the New Jersey Agricultural Experiment Station. This is publication number D-10567-2-98 of the New Jersey Agricultural Experiment Station.

* To whom correspondence should be addressed. Telephone: (732) 932-9611, ext 231. Fax: (732) 932-6776. E-mail: ludescher@aesop.rutgers.edu.

S0006-2960(98)01240-9 CCC: $15.00
Published on Web 09/25/1998

Most studies of F-actin dynamics have focused in on the flexural (bending) flexibility of the filament, since this dynamic property is believed to be important for actin's ability to carry out its diverse functions in both muscle and nonmuscle cells (*17*, *20*). The torsional flexibility of the filament, however, has not been adequately addressed despite important functional implications for the formation of bonds that hold bundles of actin filaments together in the microvilli, for the formation of actin bundles in limulus sperm, and for any as yet undefined role in actomyosin function (*16*, *21*). In addition, Tsuda et al. (*22*) have demonstrated that the actin filament is more sensitive to torsional twisting than it is to bending. Since the studies summarized above have indicated that the observed structural differences do not show up as bending flexibility differences, we hypothesize that these structural differences may manifest themselves as differences in torsional flexibility.

We have thus set out to monitor the torsional flexibility of F-actin as a function of the identity of the tightly bound divalent cation (Ca^{2+} or Mg^{2+}) or the specific nucleotide (ADP or ATP) present in G-actin prior to polymerization, the solution ionic strength, and the presence of the filament-stabilizing ligand phalloidin. The torsional flexibility of F-actin was monitored by measuring the steady-state phosphorescence emission anisotropy of the phosphorescent probe erythrosin-5-iodoacteamide covalently attached to Cys-374 of G-actin. The phosphorescence emission anisotropy is sensitive to rotational motions taking place in the actin filament on the micro- to millisecond time scale. Previous studies (*23*, *24*) have established that the microsecond rotational motions that take place in F-actin are dominated by torsional twisting motions. Our measurements indicate that the torsional dynamics of actin filaments are remarkably sensitive to the chemical structure of the divalent cation−nucleotide complex bound at the active site cleft.

MATERIALS AND METHODS

Protein Preparation and Labeling. Actin was isolated from acetone powder prepared from the leg and back muscles of New Zealand white rabbits of either sex as per established protocols (*25*). G-Actin was isolated from acetone powder by extraction into G-buffer (GB) [1 mM EPPS,[1] 0.2 mM $CaCl_2$, 1 mM NaN_3, and 0.2 mM ATP (pH 8.5)] containing 0.5 mM DTT as described by Thomas et al. (*26*); such a procedure generates G-actin with Ca^{2+} at the high-affinity site (G-Ca^{2+}-actin). Actin was stored as filaments with continuous dialysis against filament buffer (FB) [10 mM MOPS, 100 mM KCl, 2 mM $MgCl_2$, 0.2 mM $CaCl_2$, 1 mM NaN_3, and 0.2 mM ATP (pH 7.0)] at 0 °C; the dialysis buffer was changed weekly. The actin concentration was determined by the absorbance at 290 nm using an extinction coefficient of 0.63 M^{-1} cm^{-1} for actin. The protein was assayed for purity using SDS−PAGE. Actin was labeled with the phosphorescent probe erythrosin-5-iodoacetamide (Molecular Probes, Inc., Eugene, OR) as per previously reported procedures (*27*) and was stored as F-actin by dialysis against FB.

F-Ca^{2+}− or F-Mg^{2+}−actin was prepared by polymerizing G-actin with FB as per established protocols (*27*) and was dialyzed against this buffer. An actin filament containing predominantly Ca^{2+} at the high-affinity divalent cation binding site, F-Ca^{2+}-actin, was prepared by polymerizing G-Ca^{2+} with a modified filament buffer containing only calcium as the divalent cation (Ca^{2+}-FB) [10 mM MOPS, 100 mM KCl, 2.2 mM $CaCl_2$, 1 mM NaN_3, and 0.2 mM ATP (pH 7.0)] and was dialyzed against this buffer. G-Actin containing Mg^{2+} at the high-affinity divalent cation binding site (G-Mg^{2+}-actin) was prepared according to the protocol of Orlova and Egelman (*10*) by incubating G-Ca^{2+} with 0.4 mM EGTA and 0.2 mM $MgCl_2$ for 10−15 min at 4 °C. G-Mg^{2+}-actin was then polymerized to F-Mg^{2+}-actin (actin filaments containing predominantly Mg^{2+} at the high-affinity divalent cation binding site) in a modified filament buffer (Mg^{2+}-FB) [10 mM MOPS, 100 mM KCl, 0.2 mM EGTA, 2.2 mM $MgCl_2$, 1 mM NaN_3, and 0.2 mM ATP (pH 7.0)].

G-Actin containing Mg^{2+} as the tightly bound divalent cation and ADP as the nucleotide (G-Mg^{2+}-ADP-actin) was prepared from G-Mg^{2+}-ATP-actin by incubating a 2 mg/mL sample with 30 units/mL hexokinase (Sigma Chemical Co., St. Louis, MO) and 2.5 mM glucose for 2 h on ice as per the protocol of Isambert et al. (*17*). F-Mg^{2+}-ADP-actin was prepared by polymerizing G-Mg^{2+}-ADP-actin with a Mg^{2+}-ADP buffer [10 mM MOPS, 100 mM KCl, 0.2 mM EGTA, 2.2 mM $MgCl_2$, 1 mM NaN_3, 0.2 mM ADP, and 5 μM Ap_5A (pH 7.0)]. F-Mg^{2+}-ADP-P_i-actin was prepared by polymerizing G-Mg^{2+}-ADP-actin in Mg^{2+}-ADP buffer containing 30 mM P_i. ADP-actin containing BeF_3^-, F-Mg^{2+}-ADP-BeF_3^--actin, was prepared by polymerizing G-Mg^{2+}-ADP-actin with Mg^{2+}-ADP buffer containing 100 μM $BeSO_4$ and 10 mM NaF as per the procedure of Isambert et al. (*17*). These proteins were stored by dialysis at 0 °C against the appropriate buffer.

Spectroscopic Measurements. Steady-state fluorescence measurements were taken on a SPEX model F1T11i spectrofluorometer (SPEX Industries, Metuchen, NJ) equipped with a 450 W high-pressure xenon lamp, single-grating excitation and emission monochromators, dual emission monochromators in a T-format, Glan-Thomson crystal polarizers on excitation and emission, and a circulating water bath for controlling the sample temperature. The instrument is under control of a microcomputer running DM3000F software (SPEX Industries). Phosphorescence measurements were taken with this instrument equipped with a pulsed, low-pressure Xe flash lamp and a model 1934C phosphorimeter attachment (SPEX Industries).

Samples for spectroscopic measurements are prepared by mixing labeled and unlabeled actin to adjust the total concentration of erythrosin to 1 μM and the total concentration of actin (labeled and unlabeled) to 0.5 mg/mL. All luminescence measurements were taken under anaerobic conditions using the enzymatic deoxygenation protocol of Horie and Vanderkooi (*28*) and at a temperature of 20 °C. Steady-state fluorescence emission anisotropy spectra were collected for both intrinsic tryptophan and the erythrosin label; tryptophan emission anisotropy over the range of 340−350 nm was measured using 295 nm excitation, while erythrosin emission anisotropy over the range of 560−570 nm was measured using 500 nm excitation. Steady-state phosphorescence emission anisotropy measurements were

[1] Abbreviations: Ap_5A, P^1,P^5-di(adenosine 5′)-pentaphosphate; DTT, dithiothreitol; EGTA, ethyleneglycol bis(β-aminoethyl ether)-*N*,*N*,*N*′,*N*′-tetraacetic acid; EPPS, *N*-(2-hydroxyethyl)piperazine-*N*′-3-propanesulfonic acid; FB, filament buffer; MOPS, 3-(*N*-morpholino)propanesulfonic acid.

taken at 684 nm with excitation at 534 nm using a time delay of 0.07 ms and integrating the emitted photons over a total time window of 1.5 ms; four polarized intensities corresponding to vertical and horizontal excitation and emission (I_{vv}, I_{vh}, I_{hv}, and I_{hh}, where the subscripts refer to the excitation and emission polarizations, respectively) were collected and used to calculate the anisotropy r with the equation $r = (R - 1)/(R + 2)$, where $R = (I_{vv}/I_{vh})(I_{hh}/I_{hv})$. Phosphorescence intensity decay measurements were taken with excitation at 534 nm and emission at 688 nm, using an initial time delay of 0.07 ms and a total decay window of 1.5 ms, and collecting intensity every 0.01 ms. Additional details are reported elsewhere (*27*, *29*). Total intensity decays were analyzed for single-exponential lifetimes using the nonlinear least-squares fitting program NFIT (Island Products, Galveston, TX); the goodness of fit was evaluated by examination of the residuals (data minus fit) and the fit χ^2. Single-exponential functions gave good fits with residuals randomly distributed around zero and χ^2 values in the range of 1−1.4.

Determination of the "True Anisotropy" of F-Actin. When there exist in solution two chemical species such as G-actin and F-actin which differ in anisotropy, the measured anisotropy of the resultant solution is the intensity-weighted sum of the anisotropies of the two species (*27*). If we designate r_M as the measured steady-state anisotropy of the actin solution and r_{GA} and r_{FA} as the anisotropies of G-actin and F-actin, respectively, which contribute fractional phosphorescence intensities of f_{GA} and f_{FA} to the solution, respectively (such that $f_{GA} + f_{FA} = 1$), then

$$r_M = f_{GA}r_{GA} + f_{FA}r_{FA} \quad (1)$$

Since we know from experiment that $r_{GA} = 0$ for steady-state phosphorescence (*27*), then

$$r_M = f_{FA}r_{FA} = (1 - f_{GA})r_{FA} \quad (2)$$

The term f_{GA} is a function of the concentrations of G-actin ([G]) and F-actin ([F]) and a term I_{FA}/I_{GA} which represents the relative phosphorescence emission intensity of F-actin versus G-actin.

$$f_{GA} = [G]/[[G] + [F](I_{FA}/I_{GA})]$$

Since the critical concentration of actin (that is, [G] in the above expression) is known to be in the range of about 0.01−0.02 mg/mL (*30*), at the concentrations of actin used in our experiments (0.2−0.5 mg/mL), f_{GA} can be approximated by the following equation:

$$f_{GA} \approx [G]/[A](I_{FA}/I_{GA}) \quad (3)$$

where [A] is the total concentration of actin. $I_{FA}/I_{GA} = 2.81$, which is estimated from the ratio of mean lifetimes of G-actin (0.099 ms) and F-actin (0.278 ms) (*27*). If the critical concentration was 0.05 mg/mL and the total actin concentration 0.5 mg/mL, the approximation of eq 3 would introduce a 6% error.

Substituting eq 3 into eq 2, we obtain the following expression relating the measured anisotropy to the total actin concentration [A]

$$r_M = r_{FA} - ([G]/[A]I_{FA}/I_{GA})r_{FA}$$

Since the concentration of G-actin in solution is the critical concentration, c_c, then

$$r_M = r_{FA} - (c_c/I_{FA}/I_{GA})r_{FA}/[A] \quad (4)$$

Thus, a plot of r_M versus 1/[A] provides a measure of the true anisotropy of the actin filament, r_{FA}, and the critical concentration, c_c.

RESULTS

Influence of the Tightly Bound Divalent Cation on F-Actin Dynamics. Previous studies indicate that the steady-state phosphorescence anisotropy of erythrosin attached to Cys-374 provides a reliable measure of the average rotational dynamics of F-actin (*27*, *29*, *31*). Time-resolved studies (*23*, *24*) have demonstrated that the optical anisotropy on the triplet time scale reflects torsional twisting motions about the long axis of the actin filament. Such an interpretation is also supported by fluorescence microscopic studies of the reptation of labeled F-actin in solutions of unlabeled actin (*32*) which show that at actin concentrations of ≥0.5 mg/mL the actin filament is embedded within a gel-like meshwork of entangled filaments that effectively constrains any end-over-end motions of the filament. We have thus used the steady-state phosphorescence anisotropy as an indicator of the average torsional motions of the filament; a theoretical treatment (*33*) indicates that it also provides a measure of the torsional rigidity of the filament.

To determine the effect of the tightly bound divalent cation on the torsional flexibility of F-actin, F-Mg^{2+}-actin and F-Ca^{2+}-actin filaments were prepared by polymerizing G-Mg^{2+}-actin or G-Ca^{2+}-actin with a solution containing either $MgCl_2$ and KCl or $CaCl_2$ and KCl, respectively. The torsional flexibilities of these filaments at 20 °C were compared to those of filaments prepared from G-Ca^{2+}-actin monomers, but polymerized with $CaCl_2$, and $MgCl_2$ and KCl; we refer to this sample as F-(Ca^{2+}/Mg^{2+})-actin. Additional filament samples were prepared in the absence of KCl by polymerizing G-Ca^{2+}-actin and G-Mg^{2+}-actin in buffers containing only the respective divalent cation but no KCl.

F-Ca^{2+}-actin and F-Mg^{2+}-actin exhibit differences in critical concentration regardless of the type or concentration of polymerizing salt used (*11*, *34*); since the phosphorescence anisotropy of G-actin is 0.0 (*27*), variable amounts of G-actin within a filament solution will introduce artifacts by lowering the measured anisotropy. The anisotropy was thus determined as a function of actin concentration so the true anisotropy of these filaments could be determined (see Materials and Methods, especially eq 4). The steady-state phosphorescence emission anisotropies at 20 °C of the various actin samples determined as a function of actin concentration are shown in Figure 1. The *y*-intercepts of the regression lines of the anisotropy versus 1/[actin] curves provide the true anisotropy of F-actin (r_{FA}), while the slope provides an estimate of the critical concentration of the actin solution (c_c) (this procedure provides a novel technique for determining the critical concentration of an actin solution).

Estimates of the critical concentrations of G-actin in each of these solutions (c_c) and of the true anisotropy of each of these types of actin filaments (r_{FA}) are summarized in Table

Table 1: Influence of Divalent Cation, KCl, and Phalloidin on the Steady-State Phosphorescence Emission Anisotropy of Erythrosin-Labeled F-Actin

F-actin	buffer	phosphorescence emission anisotropy (r_{FA})	phosphorescence lifetime (ms)	critical concentration (μM)
F-Ca^{2+}-actin	Ca^{2+}-FB	0.083 ± 0.002[a]	0.306 ± 0.005[b]	1.6 ± 0.39[e]
F-Mg^{2+}-actin	Mg^{2+}-FB	0.066 ± 0.002[a]	0.263 ± 0.005[b]	–[d]
F-(Ca^{2+}/Mg^{2+})-actin	FB	0.084 ± 0.002[a]	0.281 ± 0.008[b]	0.62 ± 0.81[e]
F-Ca^{2+}-actin	Ca^{2+}-FB (no KCl)	0.083 ± 0.002[a]	0.334 ± 0.008[b]	1.8 ± 0.14[e]
F-Mg^{2+}-actin	Mg^{2+}-FB (no KCl)	0.066 ± 0.002[a]	0.305 ± 0.007[b]	0.39 ± 0.34[e]
Ph-F-Ca^{2+}-actin	Ca^{2+}-FB	0.098 ± 0.005	0.293 ± 0.004[c]	–[d]
Ph-F-Mg^{2+}-actin	Mg^{2+}-FB	0.080 ± 0.005	0.271 ± 0.005[c]	–[d]
Ph-F-(Ca^{2+}/Mg^{2+})-actin	FB	0.102 ± 0.006	0.276 ± 0.004[c]	–[d]

[a] From intercept on the *y*-axis of the regression line in Figure 1. [b] Mean ± standard deviation over the actin concentrations in Figure 1. [c] Mean ± standard deviation of at least three replicates. [d] Unable to determine the critical concentration due to zero slope. [e] Mean ± standard deviation based on propagation of errors calculated from the slopes of lines in Figures 1 and 2.

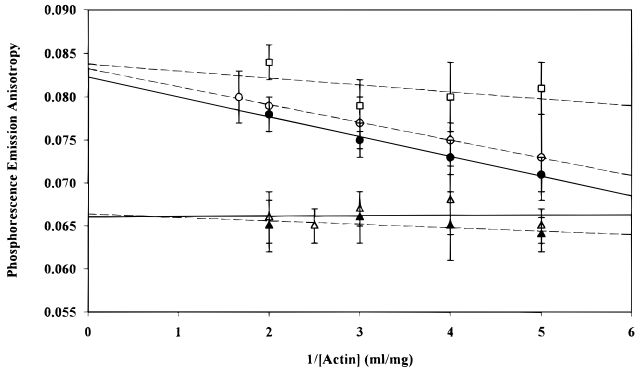

FIGURE 1: Measured steady-state phosphorescence emission anisotropy (r_M) of various F-actin solutions plotted as a function of the reciprocal of the actin concentration (see Materials and Methods, eq 4, and the text for details): (□) F-(Ca^{2+}/Mg^{2+})-actin polymerized in FB, (○ and ●) F-Ca^{2+}-actin polymerized in Ca^{2+}-FB and Ca^{2+}-FB (no KCl), respectively, and (△ and ▲) F-Mg^{2+}-actin polymerized in Mg^{2+}-FB and Mg^{2+}-FB (no KCl), respectively.

1. The critical concentration of F-Ca^{2+}-actin polymerized with $CaCl_2$ and KCl was 1.6 μM, and that of F-Ca^{2+}-actin polymerized with only $CaCl_2$ was 1.8 μM; both values were considerably larger than the critical concentration of F-Mg^{2+}-actin polymerized with only $MgCl_2$ (0.4 μM) or that of F-(Ca^{2+}/Mg^{2+})-actin polymerized with $CaCl_2$, $MgCl_2$, and KCl (0.6 μM). (The critical concentration of F-Mg^{2+}-actin polymerized with Mg^{2+} and KCl could not be determined from this analysis; however, the absence of a concentration effect in the presence of Mg indicates that the concentration of free monomer is probably <0.2 μM.) These critical concentration values are consistent with previously reported values for actin (*34*).

For both F-Ca^{2+}-actin and F-Mg^{2+}-actin, the presence of KCl in the polymerizing buffer had no effect on the filament anisotropy (Table 1). The true emission anisotropy of F-Ca^{2+}-actin was 0.083; this value was essentially identical to the anisotropy of F-(Ca^{2+}/Mg^{2+})-actin polymerized with both $MgCl_2$ and $CaCl_2$ ($r_{FA} = 0.084$) and significantly larger than the anisotropy of F-Mg^{2+}-actin ($r_{FA} = 0.066$). Since both F-Ca^{2+}-actin and F-(Ca^{2+}/Mg^{2+})-actin were polymerized from G-Ca^{2+}-actin while F-Mg^{2+}-actin was polymerized from G-Mg^{2+}-actin, this result suggests that the type of divalent cation (Ca^{2+} or Mg^{2+}) bound to the high-affinity site in G-actin prior to polymerization directly influenced the torsional flexibility of the resultant actin filament; filaments polymerized from G-Mg^{2+}-actin had a lower anisotropy and thus exhibited more torsional flexibility than filaments polymerized from G-Ca^{2+}-actin. The comparable values of anisotropy obtained for F-Ca^{2+}-actin and F-(Ca^{2+}/Mg^{2+})-actin indicate that the presence of either a single species of divalent cation (Ca^{2+} in the case of F-Ca^{2+}-actin) or a heterogeneous mixture of cations [Ca^{2+} and Mg^{2+} in the case of F-(Ca^{2+}/Mg^{2+})-actin] in the polymerizing buffer had no measurable effect on the torsional flexibility of F-actin.

Possible Ambiguities in the Interpretation of the Phosphorescence Anisotropy. The steady-state phosphorescence anisotropy is sensitive to spectroscopic properties of the probe in addition to the torsional twisting of F-actin; these include independent motions of the probe on the surface of actin, the phosphorescence lifetime of the probe, and the orientation of the triplet emission dipole of the probe with respect to the long axis of the filament (*29*, *31*). Although fluorescence anisotropy measurements indicate that erythrosin is tightly bound to the surface of F-(Ca^{2+}/Mg^{2+})-actin (*27*), we tested the possibility that the divalent cation modulates the probe mobility by measuring the steady-state fluorescence emission anisotropy of the erythrosin probe in F-Mg^{2+}-actin, F-Ca^{2+}-actin, and F-(Ca^{2+}/Mg^{2+})-actin; the results, shown in Table 2, suggest that the type of cation bound to actin did not modulate the independent motions of the probe. This conclusion was also supported by phosphorescence excitation and emission intensity scans (data not shown); these scans, which were identical for all forms of F-actin, showed no measurable influence of divalent cation on the local polarity and chemical environment of the probe. Measurements of the fluorescence anisotropy of the four actin tryptophans (Table 2) also suggested that the divalent cation did not modulate the internal dynamics of domain 1 of actin (where these residues are located) (*2*), the domain to which erythrosin is attached (at Cys-374).

The steady-state phosphorescence anisotropy of a rod-like molecule undergoing torsional twisting motions (that is, F-actin) is indexed by the ratio of the phosphorescence lifetime (τ) to a torsional twisting time (ϕ) which is directly proportional to the torsional rigidity (κ_T) (*33*); changes in the lifetime will thus modulate the measured anisotropy. We

Table 2: Influence of Divalent Cations on the Steady-State Fluorescence Emission Anisotropy of Extrinsic Erythrosin Probe and Intrinsic Tryptophans in F-Actin

F-actin	polymerizing buffer	erythrosin anisotropy (r_f at 560−570 nm)[a]	tryptophan anisotropy (r_f at 340−350 nm)[a]
F-Mg^{2+}-actin	Mg^{2+}-FB (no KCl)	0.340 ± 0.004	0.159 ± 0.004
F-Ca^{2+}-actin	Ca^{2+}-FB (no KCl)	0.340 ± 0.003	0.153 ± 0.005
F-(Ca^{2+}/Mg^{2+})-actin	FB	0.339 ± 0.004	0.162 ± 0.004

[a] Mean ± standard deviation of at least three replicates averaged over the emission wavelength range indicated.

Table 3: Influence of Added $CaCl_2$ on the Phosphorescence Emission Anisotropy of Preformed F-Mg^{2+}-Actin in the Presence and Absence of KCl

sample buffer	phosphorescence emission anisotropy[a]	phosphorescence lifetime[a] (ms)
Mg^{2+}-FB		
F-Mg^{2+}-actin	0.069 ± 0.004	0.268 ± 0.003
F-Mg^{2+}-actin and 0.6 mM $CaCl_2$	0.069 ± 0.004	0.272 ± 0.004
F-Mg^{2+}-actin and 2 mM $CaCl_2$	0.072 ± 0.004	0.277 ± 0.003
Mg^{2+}-FB (no KCl)		
F-Mg^{2+}-actin	0.068 ± 0.003	0.290 ± 0.005
F-Mg^{2+}-actin and 2 mM $CaCl_2$	0.072 ± 0.002	0.293 ± 0.003

[a] Mean ± standard deviation of at least three replicates; anisotropy displayed no concentration dependence.

measured the average phosphorescence lifetime of F-actin under various solution conditions; the results are summarized in Table 1 for all of the conditions discussed above. The average lifetime varies slightly depending upon the specific conditions of polymerization; F-Ca^{2+}-actin, for example, has a longer lifetime than F-Mg^{2+}-actin, and the presence of KCl in the polymerization buffer appears to increase the probe lifetime on both F-Ca^{2+}-actin and F-Mg^{2+}-actin. Although these changes complicate any absolute interpretation of changes in anisotropy in terms of changes in torsional rigidity (*33*), the differences in anisotropy cannot be explained away as differences in lifetime only. For example, the shorter lifetime of F-Mg^{2+}-actin compared to that of F-Ca^{2+}-actin (0.263 vs 0.306 ms) would, the torsional rigidities being equal, result in an increase in phosphorescence anisotropy rather than the decrease seen; this argument suggests that the difference in anisotropy in this case is actually an underestimate of the difference in torsional motion. However, the increases in lifetime induced by KCl in both F-Ca^{2+}-actin and F-Mg^{2+}-actin (Table 1) suggest that the similarities in anisotropy actually obscure possible differences in torsional motion between the filaments.

Effect of Phalloidin on the Torsional Flexibility of F-Mg^{2+}-Actin and F-Ca^{2+}-Actin. Phalloidin, a fungal toxin that binds to the surface of the actin filament, reduces the critical concentration to very low values (*35*) and appears to stabilize the actin filament by strengthening the bonds across and along the two-start helix (*6*). Previous studies indicate that phalloidin induces an increase in steady-state anisotropy and thus decreases the torsional twisting motions of F-actin (*27*); to determine the effect of phalloidin stabilization on the torsional flexibility, F-Ca^{2+}-actin and F-Mg^{2+}-actin were prepared in the presence of a 3-fold molar excess of phalloidin. The steady-state phosphorescence emission anisotropies of these two types of filaments were compared to that of phalloidin-stabilized F-(Ca^{2+}/Mg^{2+})-actin; the results are presented in Table 1. Phalloidin-stabilized Ca^{2+}-containing actin filaments, Ph-F-Ca^{2+}-actin with an r_{FA} of 0.098 and Ph-F-(Ca^{2+}/Mg^{2+})-actin with an r_{FA} of 0.102, had similar phosphorescence emission anisotropies, and both were higher than that of phalloidin-stabilized Ph-F-Mg^{2+}-actin (r_{FA} = 0.080); phalloidin had little or no effect on the phosphorescence lifetime of the probe (compare data in Table 1). These results indicate that although phalloidin binding increased the torsional rigidity of F-Ca^{2+}-actin and F-Mg^{2+}-actin, it did not eliminate their inherent differences in torsional flexibility brought on by the presence of different divalent cations.

Effect of Addition of $CaCl_2$ to Preformed F-Mg^{+2}-Actin Filaments. To determine whether the presence of $CaCl_2$ in solution modulates the flexibility of preformed F-Mg^{2+}-actin, we studied the effect of added $CaCl_2$ on the anisotropy of F-Mg^{2+}-actin prepared from G-Mg^{2+}-actin and polymerized with either $MgCl_2$ and KCl or only $MgCl_2$. The results, summarized in Table 3, indicate that the addition of $CaCl_2$ to preformed F-Mg^{2+}-actin filaments does not increase the phosphorescence anisotropy of F-Mg^{2+}-actin either in the presence or in the absence of KCl, and thus suggests that addition of $CaCl_2$ to performed F-Mg^{2+}-actin filaments cannot decrease the torsional flexibility of the filament. This result is consistent with the known very slow exchange kinetics of the tightly bound divalent cation in F-actin (*11*, *36*, *37*).

Influence of the Bound Nucleotide on F-Actin Dynamics. To determine whether the torsional flexibility of F-actin was dependent on the state of the nucleotide bound at the high-affinity site in actin, G-Mg^{2+}-actin with bound ADP was polymerized with $MgCl_2$ and KCl to form F-Mg^{2+}-ADP-actin filaments, with $MgCl_2$, KCl, and P_i to form F-Mg^{2+}-ADP-P_i-actin filaments, and with $MgCl_2$, KCl, and BeF_3^- to form F-Mg^{2+}-ADP-BeF_3^--actin filaments; BeF_3^- is thought to mimic the phosphate group in F-actin (*38*−*40*). The anisotropy of these filaments was independent of the actin concentration (Figure 2), indicating that the critical concentration was too small to determine using this technique; the values reported in Table 4 are thus the averages of the measurements made at three different concentrations. Although ADP-actin is expected to have a higher critical concentration than ATP-actin (*30*), the similarity in the slopes of the plots of the F-Mg^{2+}-actin solutions polymerized in

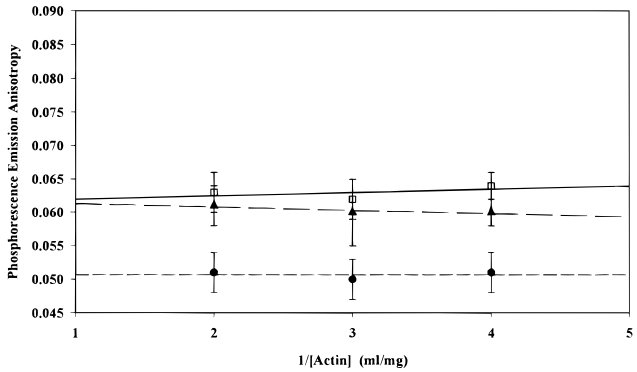

FIGURE 2: Measured steady-state phosphorescence emission anisotropy (r_M) of various F-actin solutions plotted as a function of the reciprocal actin concentration (see Materials and Methods, eq 4, and the text for details): (●) F-Mg^{2+}-ADP-actin polymerized in Mg^{2+}-ADP buffer, (□) F-Mg^{2+}-ADP-P_i-actin polymerized in Mg^{2+}-ADP buffer containing 30 mM P_i, and (▲) F-Mg^{2+}-ADP-BeF_3^--actin polymerized in Mg^{2+}-ADP buffer containing 100 μM $BeSO_4$ and 10 mM NaF.

Table 4: Influence of Nucleotide, Nucleotide Analogue, and Phalloidin on the Steady-State Phosphorescence Emission Anisotropy of F-Actin

F-actin	phosphorescence emission anisotropy	phosphorescence lifetime (ms)
F-Mg^{2+}-ADP-actin	0.051 ± 0.003^a	0.271 ± 0.009^a
F-Mg^{2+}-ADP-P_i-actin	0.063 ± 0.003^a	0.272 ± 0.007^a
F-Mg^{2+}-ADP-BeF_3^--actin	0.060 ± 0.003^a	0.282 ± 0.009^a
Ph-F-Mg^{2+}-ADP-actin	0.064 ± 0.003^b	0.275 ± 0.002^b
Ph-F-Mg^{2+}-ADP-P_i-actin	0.077 ± 0.002^b	0.277 ± 0.002^b

[a] Mean ± standard deviation over the three actin concentrations in Figure 2. [b] Mean ± standard deviation of at least three replicates.

the presence of either ATP (Figure 1) or ADP (Figure 2) suggests that divalent cation plays a dominant role in determining the critical concentration (*11*). The anisotropy of F-Mg^{2+}-actin polymerized from G-Mg^{2+}-actin in the presence of ADP (F-Mg^{2+}-ADP-actin, $r_{FA} = 0.051$) was significantly lower than the anisotropy of the same filaments polymerized in the presence of ATP (F-Mg^{2+}-actin, $r_{FA} = 0.066$, Table 1). However, the binding of either inorganic phosphate (P_i) or BeF_3^- at the active site of actin increased the anisotropy to 0.063 and 0.060, respectively, values nearly identical to that found for filaments polymerized in the presence of ATP and thus containing predominately ADP and P_i at the active site ($r_{FA} = 0.066$). Control experiments indicated that the probe phosphorescence lifetimes (compare data in Table 4), fluorescence anisotropy (data not shown), and phosphorescence excitation and emission scans (data not shown) were identical within the measurement error in the different filament forms. These data thus indicate that the state of the nucleotide bound to actin modulates the torsional flexibility of actin filaments; specifically, the presence of P_i at the active site appears to decrease the torsional flexibility of actin filaments.

The influence of phosphate bound at the active site on the torsional dynamics of F-actin persisted in the presence of a 3-fold molar excess of phalloidin. The addition of phalloidin to either F-Mg^{2+}-ADP or F-Mg^{2+}-ADP-P_i filaments increased their phosphorescence emission anisotropy (Table 4), indicative of an overall decrease in their torsional flexibility, yet did not eliminate their inherent differences in flexibility. Once again, phalloidin had no effect on the probe phosphorescence lifetime, indicating that the differences in anisotropy reflected real differences in filament torsional flexibility.

DISCUSSION

Effect of Divalent Cations. Orlova and Egelman (*10*, *12*), on the basis of image analysis of electron micrographs of actin filaments, observed structural differences in actin filaments differing in the nature of the tightly bound divalent cation (Ca^{2+} or Mg^{2+}). On the basis of these structural differences, they proposed differences in bending flexibility associated with cation binding. However, dynamic studies of actin filament bending flexibility based upon either video observation of the bending of individual fluorescence-labeled filaments (*16*, *17*) or bending of negatively stained filaments in electron micrographs (*52*) do not confirm these proposals. Since the observed structural differences do not appear to show up as bending flexibility differences, we were interested in investigating the extent to which the structural differences in F-actin observed by Orlova and Egelman (*10*, *12*) manifest themselves as torsional flexibility differences. Such a viewpoint is supported by recent measurements indicating that the torsional rigidity of F-Ca^{2+}-actin was nearly triple that of F-Mg^{2+}-actin (*16*).

The torsional flexibility of actin filaments under a variety of solution conditions was evaluated by monitoring the steady-state phosphorescence emission anisotropy of erythrosin-labeled actin. We observed that the anisotropy and hence the torsional flexibility of actin filaments are sensitive to the type of tightly bound divalent cation (Ca^{2+} or Mg^{2+}) present in G-actin prior to polymerization. When Mg^{2+} is present at the high-affinity site, the actin filaments have a lower anisotropy and are thus torsionally more flexible than when Ca^{2+} is present. These torsional flexibility differences can be reconciled with the observed structural differences as follows. Orlova and Egelman (*10*, *12*) proposed that the greater bending flexibility of Mg^{2+}-containing actin filaments was due to a loss of structural connectivity between monomers both across and along the two long-pitch helical strands. We speculate that this reduction in structural connectivity in the case of F-Mg^{2+}-actin would result in there being a greater possible extent of angular disorder of the monomers in the filament. A greater extent of monomer disorder in F-Mg^{2+}-actin would manifest itself in an increase in torsional flexibility.

Our conclusions are consistent with those of Yasuda et al. (*16*), who concluded, on the basis of observations of rotational fluctuations in video images of actin filaments held in an optical trap, that rhodamine−phalloidin stabilized Mg^{2+}-containing actin filaments were three times less torsionally rigid than Ca^{2+}-containing filaments. Our data clearly support their conclusions that the torsional flexibility of actin filaments depends on the type of tightly bound divalent cation bound at the high-affinity site in G-actin prior to polymerization. It is important to note, however, that the conclusions of Yasuda et al. are based on video observation of large-scale rotational fluctuations on the millisecond to second time scale, while the conclusions reported here are based on measurements made on the much faster micro- to millisecond time scale and thus probably reflect more localized rotational motions of the actin filament.

In the preparation of actin filaments from monomers containing different divalent cations, various polymerization buffers can be used. The monomers can be polymerized with millimolar concentrations of the respective divalent cation, with physiological concentrations of monovalent cations (KCl), or by using a combination of both monovalent and divalent cations. Strzelecka-Golaszewska et al. (*41*) have noted that the choice of the polymerization buffer could influence the flexibility of the resulting actin filament. In particular, they observed that the flexibility of the actin filament is sensitive to not only the divalent cation present in solution but also the ionic strength of the solution. However, our results indicate that the torsional flexibility of both Ca^{2+}-containing and Mg^{2+}-containing actin filaments is similar irrespective of the presence or absence of 100 mM KCl in the polymerizing buffer.

Although we observed changes in the probe lifetimes for filaments polymerized in the presence or absence of KCl, and these lifetime differences could obscure possible real differences in torsional flexibility as detected by phosphorescence anisotropy (*29*), we believe that these marginal changes in lifetime do not impact significantly our interpretation for reasons outlined in the Results. These small changes in lifetime could arise from subtle changes in the actin monomer conformation as a consequence of different cations being bound to the low-affinity sites. Selden et al. (*42*) have observed that monovalent cations (K^+) and divalent cations (Ca^{2+} or Mg^{2+}) compete for the low-affinity sites in monomeric actin and this in turn influences the affinity of actin for the divalent cation at the high-affinity site. Thus, the presence or absence of monovalent cations in solution (rather than their concentration) could result in local conformational differences which show up as lifetime changes but not as global differences in torsional flexibility. However, these conformational differences did not manifest themselves as differences in the fluorescence emission anisotropy of either the triplet probe or the four intrinsic tryptophans or in the excitation or emission spectra of the triplet probe.

Isambert et al. (*17*) observed the bending fluctuations of fluorescently labeled filaments using video microscopy and found that in the range of KCl concentrations from 0 to 100 mM the actin bending flexibility was not dependent on the ionic strength of the solution. Our results indicate that the torsional flexibility of both Ca^{2+}-containing and Mg^{2+}-containing actin filaments also does not depend on the concentration of KCl in solution over this range.

In addition to the type of divalent cation present in G-actin prior to polymerization, and to the ionic strength of the buffer, structural studies have indicated that the presence of two types of divalent cations (Ca^{2+} and Mg^{2+}) in the polymerizing buffer can also affect the torsional flexibility of the resulting F-actin filament. Orlova and Egelman (*12*) and Orlova et al. (*13*) observed using electron microscopy that when G-Ca^{2+}-actin monomers are polymerized in a buffer containing $MgCl_2$, which results in there being two types of divalent cations in solution, the resulting F-actin solution has two populations of actin filaments. One group of filaments exhibited structural features similar to those of flexible F-Mg^{2+}-actin filaments, and the other group had structural features similar to those of F-Ca^{2+}-actin filaments. The relative proportions of each of these two filament populations would be dictated by the relative amounts of each of the two types of divalent cations in solution. Our results indicate that when Ca^{2+} monomers are polymerized in the presence of either a single species of divalent cation (F-Ca^{2+}-actin) or a heterogeneous mixture of divalent cations [F-(Ca^{2+}/Mg^{2+})-actin], the resulting F-actin filaments have similar values of steady-state anisotropy and hence torsional flexibility. The similarity of the anisotropy of F-(Ca^{2+}/Mg^{2+})-actin and F-Ca^{2+}-actin leads us to the conclusion that no exchange of Ca^{2+} for Mg^{2+} occurred when Ca^{2+} monomers were polymerized in a medium containing a mixture of divalent cation, and hence the F-(Ca^{2+}/Mg^{2+})-actin filaments contained Ca^{2+} at the high-affinity site.

This apparent, albeit slight, disparity between the structural studies of Egelman and colleagues and our dynamical studies could be due to the fact that the buffer used here to polymerize F-(Ca^{2+}/Mg^{2+})-actin contained 0.2 mM $CaCl_2$ in addition to 100 M KCl and 2 mM $MgCl_2$. The presence of 0.2 mM $CaCl_2$ probably prevented the Ca^{2+} in G-actin from being exchanged with the Mg^{2+} in solution during the polymerization process. In addition, it is known that the presence of monovalent cations in the buffer can influence the exchange kinetics of the divalent cation. When only Mg^{2+} is used to polymerize G-Ca^{2+}-actin, more than 90% of the tightly bound cation is Mg^{2+} (*43*), whereas when both KCl and Mg^{2+} are included in the polymerizing buffer, the extent of exchange drops to 66% (*36*). Thus, the combined presence of KCl and $CaCl_2$ along with $MgCl_2$ in the buffer possibly precluded any exchange of divalent cation in the case of F-(Ca^{2+}/Mg^{2+})-actin. Our conclusions indicating that the presence of a heterogeneous mixture of divalent cations in the buffer does not affect the exchange of tightly bound Ca^{2+} in actin filaments are similar to those of Yasuda et al. (*16*). They observed that in the preparation of F-Ca^{2+}-actin filaments, the presence of 1 mM $MgCl_2$ in the polymerizing buffer did not result in an exchange of Ca^{2+} for Mg^{2+} in these filaments.

Once filaments are formed, however, could the tightly bound divalent cation exchange with the divalent cations present in the medium? In the answer to this question, the structural data are equivocal. Orlova and Egelman (*10*) observed that small amounts of Ca^{2+}, when added to flexible F-Mg^{2+}-actin filaments, increased the rigidity of these flexible filaments, probably via exchange of the tightly bound divalent cation. However, studies by Kasai and Oosawa (*37*) and Gershman et al. (*36*) have indicated that there is virtually no exchange of the tightly bound divalent cation in F-actin. Our results demonstrate that addition of either 0.6 or 2 mM $CaCl_2$ to preformed F-Mg^{2+}-actin filaments (polymerized with or without 0.1 M KCl) did not affect the steady-state phosphorescence emission anisotropy of these filaments, and thus did not modulate their torsional flexibility. This suggests that over a period of 2−4 h there is virtually no exchange of the tightly bound divalent cation in the actin filament.

Effect of Phalloidin. Structural studies have determined that the binding of phalloidin to actin filaments stabilizes the filaments by strengthening monomer−monomer bonds both across and along the two-start helix (*6*). However, dynamic studies of the effect of phalloidin on F-actin flexibility are not unanimous in their conclusions. Ludescher and Liu (*27*) found that the binding of phalloidin increased

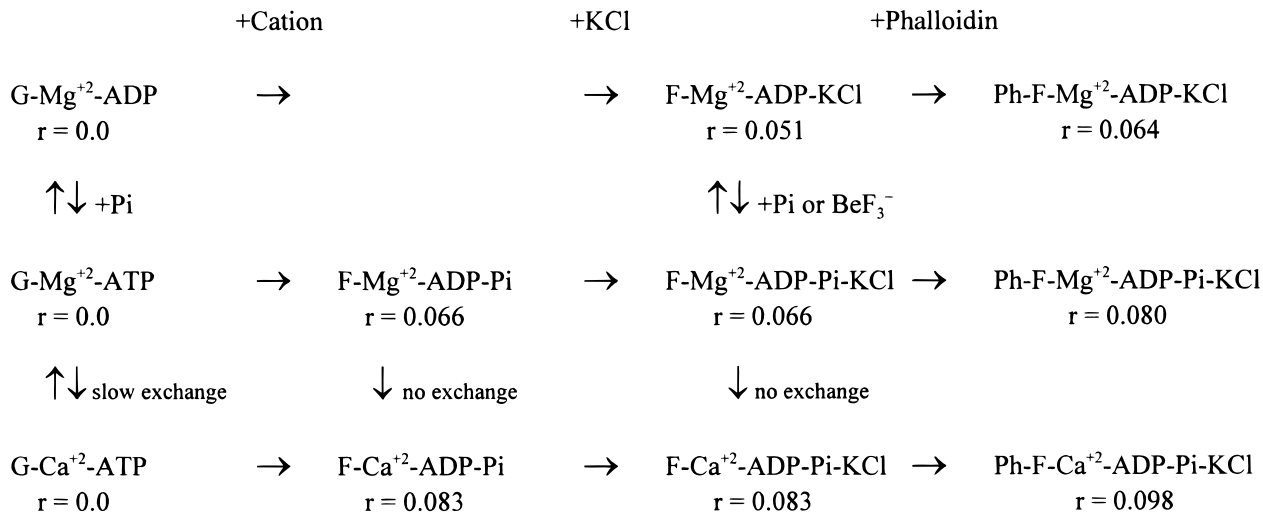

FIGURE 3: Dynamical states of the actin filament. The steady-state phosphorescence anisotropy of each state is indicated.

the steady-state phosphorescence anisotropy, thus decreasing the torsional flexibility of erythrosin-labeled F-actin. However, measurements in the micro- to millisecond time range of the transient absorption anisotropy of eosin-labeled F-actin (*23*) and of the time-resolved phosphorescence emission anisotropy of erythrosin-labeled F-actin (*24*) showed that the binding of phalloidin to actin filaments either had little effect on the torsional twisting motions of the filament (*23*) or actually increased the torsional flexibility of the filament (*24*). Our steady-state measurements clearly indicate (this work and ref *27*) that phalloidin decreased the microsecond torsional flexibility of actin filaments irrespective of whether Ca^{2+} or Mg^{2+} was bound at the high-affinity site. This suggests that phalloidin rigidifies the actin filament, probably as a result of the strengthened monomer−monomer bonds mentioned above. We have no ready explanation for the discrepancy between our work and that previously reported (*23*, *24*).

Orlova and Egelman (*10*) have indicated a differential stabilizing effect of phalloidin on actin filaments depending upon whether Ca^{2+} or Mg^{2+} is present at the high-affinity site. Phalloidin-stabilized Mg^{2+}-actin filaments exhibited structural features different from those of unstabilized Mg^{2+}-actin filaments, but similar to those of unstabilized Ca^{2+}-actin filaments. This suggests that the addition of phalloidin to Mg^{2+}-containing actin filaments increased the structural stability of these filaments so it resembles that of Ca^{2+}-containing filaments. However, their image analyses indicated that the binding of phalloidin to Ca^{2+}-actin filaments produced no structural changes, indicating no net stabilizing effect of phalloidin on Ca^{2+}-containing filaments. Our results agree with the structural studies of Orlova and Egelman (*10*) in that the phalloidin-stabilized F-Mg^{2+}-actin (Ph-F-Mg^{2+}-actin) had an anisotropy and hence a torsional flexibility comparable to that of unstabilized F-Ca^{2+}-actin. Although Orlova and Egelman (1993) proposed that the structural differences they observed would manifest themselves as bending flexibility differences, their results are actually in good agreement with our torsional flexibility results.

Effect of Nucleotide. The influence that the bound nucleotide (ATP or ADP) has on F-actin flexibility has been under scrutiny ever since Janmey et al. (*15*) first reported that actin filaments polymerized from ADP monomers exhibited structural, mechanical, and dynamical properties different from those of filaments polymerized from ATP monomers. Similar conclusions regarding actin filament flexibility as a function of the bound nucleotide were reached by Orlova and Egelman (*10*) in their structural studies. However, their findings were ambiguous because their ATP monomers and ADP monomers had different divalent cations present at the high-affinity site. However, Pollard et al. (*19*) arrived at different conclusions on the basis of a comparison of electron micrographs and the rheological properties of F-actin polymerized from either ATP- or ADP-G-actin; they observed that actin filaments polymerized from either ATP or ADP monomers did not exhibit any gross structural or mechanical differences. However, they did not rule out the possibility that there could exist subtle differences in the packing of the monomers in the actin helix in the case of filaments differing in the type of bound nucleotide. In addition, Isambert et al. (*17*) observed that video images of Mg^{2+}-containing actin filaments exhibited similar persistence lengths independent of the bound nucleotide, suggestive of comparable bending flexibilities.

Our results indicate that Mg^{2+}-containing actin filaments polymerized from ADP monomers have a lower steady-state phosphorescence emission anisotropy and hence greater torsional flexibility than filaments polymerized from ATP monomers. This suggests that the type of nucleotide present in monomeric actin prior to polymerization directly influences the torsional flexibility of the resulting filament. In addition, we have observed that the binding of P_i or its high-affinity analogue BeF_3^- induced an increase in the anisotropy of these flexible ADP-containing filaments to a value comparable to that of the ATP-containing filaments. These conclusions are in agreement with previous structural studies wherein it has been proposed that the release of phosphate following ATP hydrolysis leads to destabilization of the filament (*30*, *43*), and that the binding of phosphate to F-ADP filaments stabilizes the filament (*39*, *44*). Our results here indicate a stabilization of the actin filament (via a reduction in its torsional flexibility) upon binding of phosphate or its high-affinity analogue BeF_3^-. These results agree in part with those of Combeau and Carlier (*39*), who observed that although both phosphate and BeF_3^- stabilized F-ADP filaments, the stabilization induced by BeF_3^- was different from

that of phosphate. On the basis of this observation, they proposed that BeF_3^- may be an analogue of the F-ADP-P* transition state rather than the F-ADP-P state. However, our results indicate a comparable degree of stabilization induced by either phosphate or BeF_3^-; from the perspective of torsional flexibility, these two anions produce the same state in the presence of ADP.

Torsional Dynamics and Possible States of F-Actin. The steady-state phosphorescence emission anisotropies of various states of the actin filament are summarized in Figure 3, providing an overview of the torsional flexibilities of the various states of the actin filament. As summarized in this scheme, F-actin is a remarkably malleable filament whose intrinsic torsional flexibility is modulated by the nature of the tightly bound divalent cation and the nucleotide present in the monomer prior to polymerization, the presence of inorganic phosphate (or BeF_3^-), and the binding of the stabilizing ligand phalloidin. The measured differences in torsional flexibility in most cases closely agree with the differences in structural connectivity seen in electron micrographs of negatively stained actin filaments by Egelman and colleagues. This suggests that the observed structural changes may provide the mechanistic basis for modulating the torsional flexibility of the filament; a looser correlation between structural differences and the bending flexibility suggests that there may only be an indirect, or a more complex, connection between these properties. Variability of torsional rigidity in the absence of comparable changes in bending ridigity suggests that the actin filament does not behave as a uniform elastic cylinder, and thus, dynamical models based on such a simplified physical model are inadequate. Our results also suggest that chemical heterogeneity within an individual filament, due to differences in the nature of the bound nucleotide or divalent cation, for example, could lead to torsional heterogeneity along the filament axis.

Functional Significance of Torsional Flexibility Differences. The functional importance of torsional flexibility of the actin filament for contractility is not adequately understood despite evidence of the presence of elasticity and/or torsional motions in the actin filament during force generation or movement. In vitro sliding studies of actin filaments over attached HMMs have demonstrated that torsional twisting motions are induced in the actin filament during ATP hydrolysis (*45*, *46*). Wakabayashi et al. (*47*) and Huxley et al. (*48*) have also reported that a large portion of the series elasticity in the muscle is due to the extensibility of the actin filament. Wakabayashi et al. (*47*) observed slight changes in actin's helical structure during isometric contraction, and Grazi et al. (*49*) observed changes in the orientation of the actin monomer in the filament upon interaction with rigor S1. These helical rearrangements of monomers in the filament would occur predominantly via angular rather than via axial changes of monomer orientation in the filament. Such angular changes would be manifest as torsional motions in the filament. This suggests that torsional motions in the actin filament could be intimately involved in the mechanism of force generation; our previous studies of actin torsional motion in the presence of S1 during ATP hydrolysis (*29*) also provide evidence of this phenomenon. Studies by Miki et al. (*50*) and more recently by Orlova and Egelman (*51*) have demonstrated that actin filaments that differ in the nature of the tightly bound divalent cation exhibit a differential interaction with myosin fragments (S1 and HMM). Much work on unraveling the complexity of actin filament dynamics and the specific role it plays in force generation remains to be done.

REFERENCES

1. Bray, D. (1992) *Cell Movements*, Garland Publishing Co., New York and London.
2. Kabsch, W., Mannhertz, H. G., Suck, D., Pai, E. F., and Holmes, K. (1990) *Nature 347*, 37−44.
3. McLaughlin, P. J., Gooch, J. T., Mannherz, H.-G., and Weeds, A. G. (1993) *Nature 364*, 685−692.
4. Schutt, C. E., Myslik, J. C., Rozycki, M. D., Goonesekere, N. C. W., and Lindberg, U. (1993) *Nature 365*, 810−816.
5. Holmes, K. C., Popp, D., Gebhard, W., and Kabsch, W. (1990) *Nature 347*, 44−49.
6. Lorenz, M., Popp, D., and Holmes, K. C. (1993) *J. Mol. Biol. 234*, 826−836.
7. Schroder, R. R., Manstein, D. J., Jahn, W., Holden, H., Rayment, I., Holmes, K. C., and Spudich, J. A. (1993) *Nature 364*, 171−174.
8. Rayment, I., Holden, H. M., Whittaker, M., Yohn, C. B., Lorenz, M., Holmes, K., and Milligan, R. A. (1993) *Science 261*, 58−65.
9. Orlova, A., and Egelman, E. H. (1992) *J. Mol. Biol. 227*, 1043−1053.
10. Orlova, A., and Egelman, E. H. (1993) *J. Mol. Biol. 232*, 334−341.
11. Estes, J. E., Selden, L. A., Kinosian, H. J., and Gersham, L. C. (1992) *J. Muscle Res. Cell Motil. 13*, 272−284.
12. Orlova, A., and Egelman, E. H. (1995) *J. Mol. Biol. 245*, 582−597.
13. Orlova, A., Prochniewicz, E., and Egelman, E. H. (1995) *J. Mol. Biol. 245*, 598−607.
14. Egelman, E., and Orlova, A. (1995) *Curr. Opin. Struct. Biol. 5*, 172−180.
15. Janmey, P. A., Hvidt, S., Oster, G. F., Lamb, J., Stossel, T. P., and Hartwig, J. H. (1990) *Nature 347*, 95−99.
16. Yasuda, R., Miyata, H., and Kinosita, K., Jr. (1996) *J. Mol. Biol. 263*, 227−236.
17. Isambert, H., Venier, P., Maggs, A. C., Fattoum, A., Kassab, R., Pantaloni, D., and Carlier, M.-C. (1995) *J. Biol. Chem. 270*, 11437−11444.
18. Burlacu, S., Janmey, P., and Borejdo, J. (1992) *Am. J. Physiol. 262*, C569−C577.
19. Pollard, T. D., Goldberg, I., and Schwarz, W. H. (1992) *J. Biol. Chem. 267* (28), 20339.
20. Oosawa, F., Fujime, S., Ishiwata, S., and Mihashi, K. (1973) *Cold Spring Harbor Symp. Quant. Biol. 37*, 277−285.
21. Stokes, D. L., and DeRosier, D. J. (1987) *J. Cell Biol. 104*, 1005−1017.
22. Tsuda, Y., Yastake, H., Ishijima, A., and Yanagida, T. (1996) *Proc. Natl. Acad. Sci. U.S.A. 93*, 12937−12942.
23. Yoshimura, H., Nishio, T., and Mihashi, K. (1984) *J. Mol. Biol. 179*, 453−467.
24. Prochniewicz, E., Zhang, Q., Howard, E., and Thomas, D. (1996) *J. Mol. Biol. 255*, 446−457.
25. Pardee, J., and Spudich, J. (1982) *Methods Enzymol. 65*, 164−181.
26. Thomas, D. D., Seidel, J. C., and Gergely, J. (1979) *J. Mol. Biol. 132*, 257−273.
27. Ludescher, R. D., and Liu, Z. (1993) *Photochem. Photobiol. 58*, 858−866.
28. Horie, T., and Vanderkooi, J. M. (1981) *Biochim. Biophys. Acta 670*, 294−297.
29. Ng, C.-M., and Ludescher, R. D. (1994) *Biochemistry 33*, 9098−9104.
30. Korn, E. D., Carlier, M.-F., and Pantaloni, D. (1987) *Science 238*, 638−644.
31. Ng, C.-M., and Ludescher, R. D. (1994) *Proc. SPIE-Int. Soc. Opt. Eng. 2137*, 448−455.

32. Kas, J., Strey, H., and Sackmann, E. (1994) *Nature 368*, 226−229.
33. Ludescher, R. D., and Ludescher, W. H. (1993) *Photochem. Photobiol. 58*, 881−883.
34. Selden, L. A., Gershman, L. C., and Estes, J. E. (1986) *J. Muscle Res. Cell Motil. 7*, 215−224.
35. Faulstich, H., Zobeley, S., Heintz, D., and Drewes, G. (1993) *FEBS Lett. 318*, 218−222.
36. Gershman, L. C., Selden, L. A., Kinosian, H. J., and Estes, J. E. (1994) in *Actin: Biophysics, Biochemistry, and Cell Biology* (Estes, J. E., and Higgins, P. J., Eds.) pp 35−49, Plenum Press, New York.
37. Kasai, M., and Oosawa, F. (1969) *Biochim. Biophys. Acta 172*, 300−310.
38. Bigay, J., Deterre, P., Pfister, C., and Chabre, M. (1985) *FEBS Lett. 191*, 181−185.
39. Combeau, C., and Carlier, M.-C. (1988) *J. Biol. Chem. 263*, 17429−17436.
40. Lepault, J., Ranck, J.-L., Erk, I., and Carlier, M.-C. (1994) *J. Struct. Biol. 112*, 79−91.
41. Strzelecka-Golaszewska, H., Wozniak, A., Hult, T., and Lindberg, U. (1996) *Biochem. J. 316*, 713−721.
42. Selden, L. A., Estes, J. E., and Gershman, L. C. (1989) *J. Biol. Chem. 264*, 9271−9277.
43. Carlier, M.-F., Pantaloni, D., and Korn, E. D. (1986) *J. Biol. Chem. 261*, 10778−10784.
44. Carlier, M.-F. (1991) *J. Biol. Chem. 266*, 1−4.
45. Tanaka, Y., Ishijima, A., and Ishiwata, S. (1992) *Biochim. Biophys. Acta 1159*, 94−98.
46. Nishizaka, T., Yagi, T., Tananka, Y., and Ishiwata, S. (1993) *Nature 361*, 269−271.
47. Wakabayashi, K., Sugimoto, Y., Tanaka, H., Ueno, Y., Takezawa, Y., and Amemiya, Y. (1994) *Biophys. J. 67*, 2422−2435.
48. Huxley, H. E., Stewart, A., Sosa, H., and Irving, T. (1994) *Biophys. J. 67*, 2411−2424.
49. Grazi, E., Magri, E., Schwienbacher, C., and Trombetta, G. (1994) *Biochem. Biophys. Res. Commun. 200*, 58−64.
50. Miki, M., Wahl, P., and Auchet, J.-C. (1982) *Biochemistry 21*, 3661−3665.
51. Orlova, A., and Egelman, E. H. (1997) *J. Mol. Biol. 265*, 469−474.
52. Steinmetz, M. O., Goldie, K. N., and Aebi, U. (1997) *J. Cell Biol. 138*, 559−574.

BI981240I